CrossMark

electronic reprint

Acta Crystallographica Section F
Structural Biology Communications
ISSN 2053-230X

Crystallization and preliminary X-ray diffraction analysis of Xyn30D from *Paenibacillus barcinonensis*

María Ángela Sainz-Polo, Susana Valeria Valenzuela, F. Javier Pastor and Julia Sanz-Aparicio

Acta Cryst. (2014). F**70**, 963–966

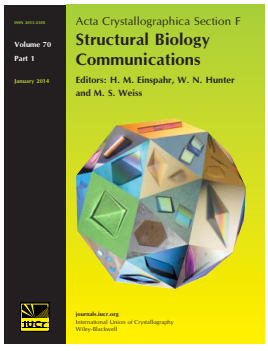

Acta Crystallographica Section F
Structural Biology Communications
ISSN 2053-230X

Crystallization and preliminary X-ray diffraction analysis of Xyn30D from *Paenibacillus barcinonensis*

María Ángela Sainz-Polo,[a] Susana Valeria Valenzuela,[b] F. Javier Pastor[b] and Julia Sanz-Aparicio[a]*

[a]Department of Crystallography and Structural Biology, Institute of Physical Chemistry 'Rocasolano', Consejo Superior de Investigaciones Científicas, Serrano 119, 28006 Madrid, Spain, and [b]Department of Microbiology, Faculty of Biology, Universitat de Barcelona, Avenida Diagonal 643, 08028 Barcelona, Spain

Correspondence e-mail: xjulia@iqfr.csic.es

Received 4 April 2014
Accepted 23 May 2014

Xyn30D, a new member of a recently identified group of xylanases, has been purified and crystallized. Xyn30D is a bimodular enzyme composed of an N-terminal catalytic domain belonging to glycoside hydrolase family 30 (GH30) and a C-terminal family 35 carbohydrate-binding domain (CBM35) able to bind xylans and glucuronic acid. Xyn30D shares the characteristic endo mode of action described for GH30 xylanases, with the hydrolysis of the β-(1,4) bonds of xylan being directed by α-1,2-linked glucuronate moieties, which have to be placed at the -2 subsite of the xylanase active site. Crystals of the complete enzyme were obtained and a full data set to 2.3 Å resolution was collected using a synchrotron X-ray source. This represents the first bimodular enzyme with the domain architecture GH30-CBM35. This study will contribute to the understanding of the role that the different xylanases play in the depolymerization of glucuronoxylan.

1. Introduction

The enzymatic degradation of the plant cell wall is a process that is attracting more interest every day because of its implications for the use of renewable carbon sources. Xylan is one of the main components of the cell wall, which encompasses one third of the world's renewable carbon (de Vries & Visser, 2001). Consequently, its depolymerization plays a key role in the biodegradation of the plant cell wall. Xylanases are enzymes that catalyze the hydrolysis of the main chain of xylan and to date they have been successfully used in the textile, food, feed and paper industries among others. Nevertheless, the complexity of xylan requires the combined action of different xylanases and other enzymes able to break the heterogeneous side-chain substitutions present in highly branched xylans (Biely, 1985).

Commonly, xylanases are generally classified into the GH10 or GH11 families of glycosyl hydrolases, but in recent times new xylanases have been classified into families GH5, GH8, GH30 and GH43 (CAZy; http://www.cazy.org/, Lombard *et al.*, 2014). The GH30 family members share the common feature of only being active on glucuronoxylans, which is a unique trait of this xylanase family. Recently, the first two xylanases belonging to this family have been crystallized: glucuronoxylan xylanohydrolase from *Bacillus subtilis* (PDB entry 3kl0; St John *et al.*, 2011) and glucuronoxylanase from *Erwinia chrysanthemi* (PDB entry 2y24; Urbanikova *et al.*, 2011). Both enzymes show a catalytic domain with a $(\beta/\alpha)_8$-barrel fold tightly connected to a side β-sheet structure. A new GH30 xylanase, *Paenibacillus barcinonensis* Xyn30D, has been identified and characterized (Valenzuela *et al.*, 2012). The enzyme is a bimodular enzyme comprised of a complete GH30 domain bound to an ancillary CBM35 carbohydrate-binding module (Montanier *et al.*, 2009; Correia *et al.*, 2010) and constitutes the first example of a modular xylanase within the GH30 family. Here, we report its purification, crystallization and preliminary X-ray crystallographic analysis.

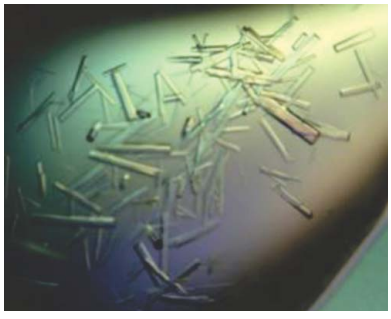

The few existing reports on the catalytic properties of xylanases specific for glucuronoxylan hydrolysis make it difficult to identify common traits that can provide clues to understanding their contribution to the depolymerization of this polysaccharide. Further studies will be required to ascertain their role in the degradation of xylan in natural habitats. Elucidation of the Xyn30D structure will contribute to deciphering the biochemical function of the different xylanases present in a single microorganism.

2. Experimental procedures

2.1. Cloning and expression of Xyn30D

Construction of the Xyn30D expression vector for crystallization studies has been described previously (Valenzuela *et al.*, 2012). The vector expressed the full-length enzyme containing its own signal peptide and linked to a C-terminal His_6 tag. For the expression assay, *Escherichia coli* BL21 Star (DE3) was transformed with pET101Xyn30D and grown in ampicillin-supplemented LB medium (50 µg ml^{-1}) at 310 K until the absorbance at 600 nm reached 0.8; it was then induced with 0.5 m*M* IPTG (isopropyl β-D-1-thiogalactopyranoside) for 18 h at 303 K. The cells were collected by centrifugation at 6000*g* for 15 min and resuspended in 50 m*M* Tris–HCl pH 7.0, 20 m*M* imidazole, 500 m*M* NaCl. Cells were disrupted with a French press. The solution was then centrifuged for 20 min at 20 000*g* and the resulting supernatant was placed on ice. Xyn30D was expressed with its own signal peptide and with its C-terminus fused to a 6×His tag to facilitate purification. The molecular mass of this construct is 62 124 Da.

2.2. Purification of Xyn30D

The recombinant Xyn30D was initially purified from cell extracts by immobilized metal-affinity chromatography (IMAC) using 1 ml HisTrap HP columns (GE Healthcare) and was eluted in 50 m*M* Tris–HCl pH 7.0, 500 m*M* NaCl with a 20–500 m*M* imidazole gradient on a fast protein liquid chromatography system (ÄKTA FPLC; GE Healthcare). The elution fractions were concentrated and dialyzed with 50 m*M* Tris–HCl pH 8.0 using Centricon centrifugal filter units of 30 kDa molecular-mass cutoff (Millipore) to a final volume of less than 10 ml. The concentrated enzyme was then loaded onto Mono Q 5/50 GL (GE Healthcare). Single injections of 1800 µl were made and the protein was eluted using 20 m*M* Tris–HCl pH 8.0 buffer with a gradient of 0–1 *M* NaCl. Purified Xyn30D was concentrated to at least 10 mg ml^{-1} in 20 m*M* Tris–HCl pH 8, 150 m*M* NaCl for crystallization screening. The purity of the protein was determined by SDS–PAGE (Laemmli, 1970).

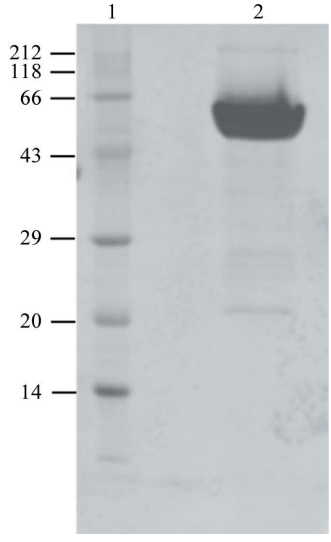

Figure 1
SDS–PAGE analysis of purified Xyn30D in 15% polyacrylamide gels. Lane 1, low-molecular-weight protein marker (labelled in kDa); lane 2, purified Xyn30D.

Table 1
Data-collection statistics for the Xyn30D crystal.

Values in parentheses are for the highest resolution shell.

Wavelength (Å)	0.873
Source	ESRF
Beamline	ID23-2
Space group	$P3_221$
Unit-cell parameters (Å)	$a = b = 173.81$, $c = 183.74$
Resolution limits (Å)	35.74–2.30 (2.42–2.30)
Unique reflections	141869 (20540)
R_{merge}†	0.149 (0.531)
Completeness (%)	99.9 (100)
Mean multiplicity	3.7 (3.7)
Mean $I/\sigma(I)$	8.7 (2.8)
Wilson *B* factor (Å^2)	17.04

† $R_{merge}(I) = \sum_{hkl}\sum_i |I_i(hkl) - \langle I(hkl)\rangle| / \sum_{hkl}\sum_i I_i(hkl)$, where $I_i(hkl)$ is the intensity of the *i*th measurement of a symmetry-related reflection with indices *hkl*.

2.3. Enzyme assays

Xyn30D was assayed for enzyme activity using the method of Somogyi and Nelson (Valenzuela *et al.*, 2012) to detect the release of reducing sugar. Beechwood xylan (Sigma) at 1.5%(*w*/*v*) was included in the reactions as the substrate.

2.4. Crystallization

In order to determine a suitable protein concentration for crystallization trials, the Pre-Crystallization Test (PCT; Hampton Research) was used and 13 mg ml^{-1} was found to be an appropriate value. Initial crystallization conditions of the purified protein samples were investigated by high-throughput techniques with a NanoDrop robot (Innovadyne Technologies Inc.) using the commercially available Index, SaltRx and Crystal Screen from Hampton Research and The PACT Suite and The JCSG+ Suite from Qiagen. The assays were carried out by the sitting-drop vapour-diffusion method at 291 K in Innovaplate SD-2 microplates (Innovadyne Technologies Inc.) by mixing 250 nl protein solution with 250 nl precipitant solution and equilibrating against 60 µl well solution.

A few PEG 3350-containing solutions gave small needle-like crystals. These conditions were optimized through further sitting-drop and hanging-drop experiments by mixing 2 µl protein solution with 1 µl precipitant solution and equilibrating against 500 µl well solution on VDX Plates (Hampton Research).

2.5. Data collection and processing

Crystals tested with synchrotron radiation were soaked in precipitant solution containing an additional 30%(*v*/*v*) glycerol (Garman & Mitchell, 1996) for a few seconds before being flash-cooled to 100 K. Diffraction data sets were collected on the ID23-2 beamline at the European Synchrotron Radiation Facility (ESRF), Grenoble, France. The data sets were processed using *iMosflm* (Battye *et al.*, 2011) and *SCALA* (Evans, 2006) as distributed in the *CCP*4 suite (Winn *et al.*, 2011).

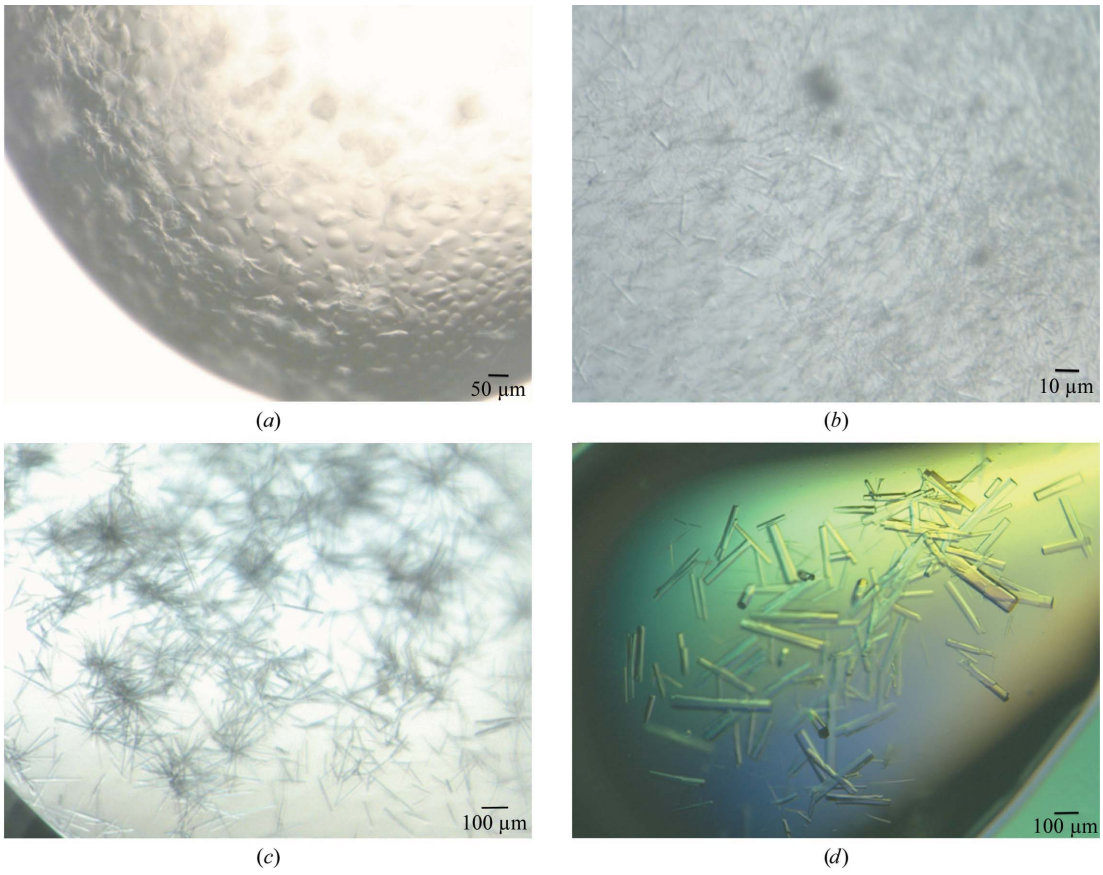

Figure 2
Xyn30D crystals obtained from (*a*) 15%(*w*/v) PEG 3350, 0.2 *M* magnesium chloride, 0.1 *M* Tris–HCl pH 8.5 (protein:precipitant ratio 1 µl:1 µl), (*b*) 14%(*w*/*v*) PEG 3350, 5%(*v*/*v*) glycerol, 0.1 *M* Tris–HCl pH 8.0 (protein:precipitant ratio 1 µl:1 µl), (*c*) 13%(*w*/*v*) PEG 3350, 5%(*v*/*v*) glycerol, 0.1 *M* Tris–HCl pH 8 (protein:/precipitant ratio 2 µl:1 µl) and (*d*) 10%(*w*/*v*) PEG 3350, 5%(*v*/*v*) glycerol, 0.1 *M* Tris–HCl pH 8.0 and streak-seeding (protein:precipitant ratio 2 µl:1 µl).

3. Results and discussion

The purification of the Xyn30D sample through two chromatographic steps yielded an active protein with a high degree of purity (Fig. 1). A preliminary search for crystallization conditions with several commercial screens led to small needle-like crystals at 15%(*w*/*v*) PEG 3350, 0.2 *M* magnesium chloride, 0.1 *M* Tris–HCl pH 8.5 (Fig. 2*a*). Optimization was pursued manually by varying the protein/precipitant concentration and pH, and by trying different additives. The crystals in Fig. 2(*b*) were obtained when glycerol was included as an additive. Further improvements in the crystals (Fig. 2*c*) resulted from changing the drop ratio (to 2 µl protein:1 µl precipitant solution). Finally, streak-seeding (Bergfors, 2003) using the small needle crystals in Fig. 2(*b*) was crucial in obtaining high-quality crystals that allowed full data collection. Thus, the best rod-shaped crystals (Fig. 2*d*) were grown by streak-seeding into drops consisting of 2 µl Xyn30D (13 mg ml^{-1}) in 20 m*M* Tris–HCl pH 8.0, 80 m*M* NaCl and 1 µl of precipitant solution [10%(*w*/*v*) PEG 3350, 5%(*v*/*v*) glycerol, 0.1 *M* Tris–HCl pH 8.0]. The optimized crystals grew within 10 d at 291 K.

The final optimized crystals were tested using a synchrotron-radiation source to obtain high-resolution data. Several native data sets were collected at 100 K on the ID23-2 beamline at the ESRF, Grenoble, France. The crystals belong to space group $P3_221$, with unit-cell parameters $a = b = 173.81$, $c = 183.74$ Å, and diffracted to 2.3 Å resolution (Fig. 3, Table 1). As calculated from its sequence analysis, the molecular mass of the monomer is 62 124 Da. Assuming a reasonable Matthews coefficient value within the range 4.87–2.44 Å^3 Da^{-1} (Matthews, 1968), corresponding to 50–70% solvent content, the presence of three to five molecules in the asymmetric unit should be expected. We investigated the local symmetry relating

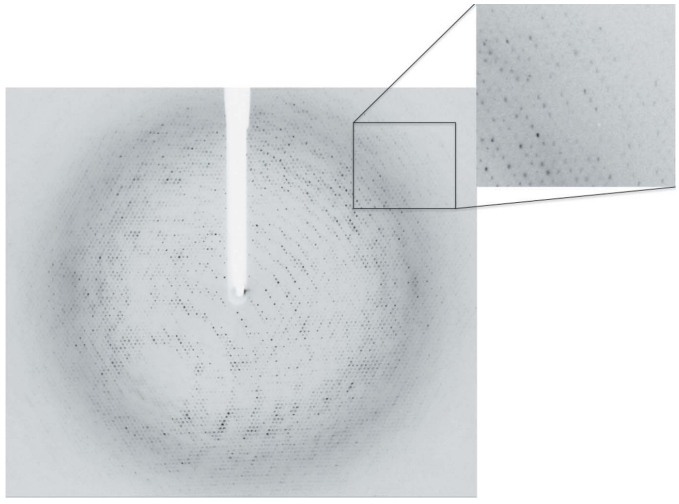

Figure 3
X-ray diffraction pattern of Xyn30D obtained using a synchrotron source. The maximum observed resolution is 2.3 Å.

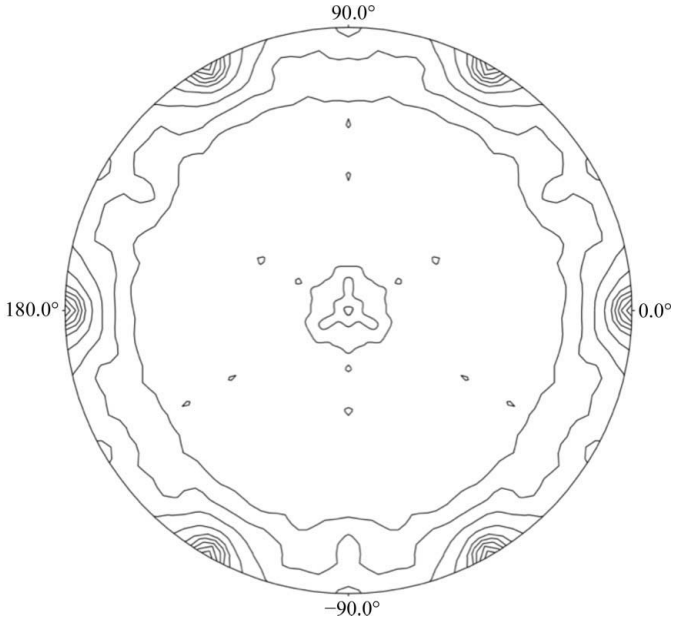

Figure 4
Plot of the self-rotation function of Xyn30D crystals in the $\kappa = 180^\circ$ section. The view is down the c axis and $\varphi = 0$ and $\varphi = 90^\circ$ correspond to the a and b^* axes, respectively.

the subunits in the asymmetric unit using *POLARRFN* (Kabsch, 1976) from the *CCP*4 package. Several self-rotation functions were computed in the resolution range 15–3.5 Å with Patterson vectors from 25 to 40 Å radius of integration. The stereographic projection of the $\kappa = 180^\circ$ section, shown in Fig. 4, revealed the presence of noncrystallographic twofold symmetry in the *ac* plane. Structure determination is in progress using two different models: firstly, the coordinates of glucuronoxylanase XynC from *B. subtilis* (St John *et al.*, 2009; PDB entry 3gtn), which shows 80% sequence identity to the GH30 portion of Xyn30D and, secondly, the C-terminal CBM35 from *Amycolaptosis orientalis* exo-chitosanase (Montanier *et al.*, 2009; PDB entry 2vzq), with 40% identity to the Xyn30D C-terminal domain. These models were used as templates in the molecular-replacement method with data to 3.5 Å resolution using *MOLREP* (Winn *et al.*, 2011). A solution containing four molecules in the asymmetric unit has been found, which is consistent with twofold NCS symmetry. Preliminary structural refinement of this tetramer with *REFMAC* (Murshudov *et al.*, 2011) decreased the R factor to 0.41 ($R_{\rm free}$ = 0.46). Model building and further refinement are ongoing.

This work was supported by grants CTQ2010-20238-C03-02 and BIO2010-20508-C04-03 from the Dirección General de Investigación MINECO. This is a product of the Project 'Factoría Española de Cristalización' Ingenio/Consolider 2010. MASP is supported by a JAE-PreDoc fellowship from CSIC. We also thank the ESRF for beamtime and ID23-2 staff for providing assistance with data collection.

References

Battye, T. G. G., Kontogiannis, L., Johnson, O., Powell, H. R. & Leslie, A. G. W. (2011). *Acta Cryst.* D**67**, 271–281.
Bergfors, T. (2003). *J. Struct. Biol.* **142**, 66–76.
Biely, P. (1985). *Trends Biotechnol.* **3**, 286–290.
Correia, M. A. *et al.* (2010). *Biochemistry*, **49**, 6193–6205.
Evans, P. (2006). *Acta Cryst.* D**62**, 72–82.
Garman, E. F. & Mitchell, E. P. (1996). *J. Appl. Cryst.* **29**, 584–587.
John, F. J. St, Godwin, D. K., Preston, J. F., Pozharski, E. & Hurlbert, J. C. (2009). *Acta Cryst.* F**65**, 499–503.
John, F. J. St, Hurlbert, J. C., Rice, J. D., Preston, J. F. & Pozharski, E. (2011). *J. Mol. Biol.* **407**, 92–109.
Kabsch, W. (1976). *Acta Cryst.* A**32**, 922–923.
Laemmli, U. K. (1970). *Nature (London)*, **227**, 680–685.
Lombard, V., Golaconda Ramulu, H., Drula, E., Coutinho, P. M. & Henrissat, B. (2014). *Nucleic Acids Res.* **42**, D490–D495.
Matthews, B. W. (1968). *J. Mol. Biol.* **33**, 491–497.
Montanier, C. *et al.* (2009). *Proc. Natl Acad. Sci. USA*, **106**, 3065–3070.
Murshudov, G. N., Skubák, P., Lebedev, A. A., Pannu, N. S., Steiner, R. A., Nicholls, R. A., Winn, M. D., Long, F. & Vagin, A. A. (2011). *Acta Cryst.* D**67**, 355–367.
Urbanikova, L., Vrsanska, M., Krogh, K. B., Hoff, T. & Biely, P. (2011). *FEBS J.* **278**, 2115–2116.
Valenzuela, S. V., Diaz, P. & Pastor, F. I. (2012). *Appl. Environ. Microbiol.* **78**, 3923–3931.
Vries, R. P. de & Visser, J. (2001). *Microbiol. Mol. Biol. Rev.* **65**, 497–522.
Winn, M. D. *et al.* (2011). *Acta Cryst.* D**67**, 235–242.